Characterization of Voltage Reference Noise for the Laser Interferometer Space Antenna

Ellery Ames
March 2008

Abstract.

Direct detection of gravitational waves will open a completely new window on our universe allowing us to observe extremely energetic events and to peer back to the first few moments after the big bang. Although gravitational waves have yet to be detected directly a planned space-based detector, to launch within about a decade, is expected to directly detect gravitational waves from many sources. These sources, which are the most energetic events in the universe, only emit very small gravitational wave signals. In order to detect these extremely small gravitational wave signals, the detector tracks the variations in the relative motions of sets of proof masses via interferometry. Even in the space environment, which is much quieter than earth, there are many sources of disturbance to the detector that must be accounted for. To account for disturbances, each spacecraft employs drag-free technology, and the sensitivity of the drag-free systems rely on the noise levels of voltage references. However, the noise of voltage references at the low frequencies of the detector measurement band is not well known. We have characterized the noise of some commercially available voltage references at the relevant frequencies, and determined the temperature dependence of these references. Results indicate that the voltage reference noise most likely cannot be reduced below the micro volt $/\sqrt{Hz}$ level, and further more, will not significantly improve in more temperature stable environments, such as space.

1. Introduction

Astrophysical observations are currently performed across the electromagnetic spectrum, from gamma rays to radio waves [1]. While electromagnetic observations have provided a wealth of insight about the universe, a new, complimentary way of looking at the universe is about to become available [2]. This will be through the detection of gravitational radiation, also known as gravitational waves. Gravitational waves are phenomena predicted by the theory of general relativity. Detection of such waves will give additional credence to general relativity and will allow for the observation of a whole new set of astrophysical phenomena.

A space-based gravitational wave detector, the Laser Interferometer Space Antenna (LISA), is currently in the advanced stages of planning and is expected to launch in about 10 years. A significant issue for LISA is obtaining the desired sensitivities in order to observe interesting gravitational wave signals. The sensitivity of the detector relies in part on low electrical noise, and one source of electrical noise is the voltage references used on the spacecraft. However, the noise of voltage references within the LISA frequency band is not well known. We have characterized the noise of several common voltage references and their temperature dependencies. Temperature measurements are discussed in section 3.3, while the noise measurements are given in Section 3.4. Sections 2.1 and 2.2 are devoted to introducing gravitational waves and LISA respectively.

2. Background

2.1. Gravitational Waves

Gravitational waves can be thought of as ripples in spacetime. According to the theory of general relativity, a massive body causes spacetime to curve, and correspondingly the curvature of spacetime affects the motions of other bodies (Figure 1). Similarly, ripples, or perturbations, in spacetime may be caused by certain motions of massive bodies (Figure 2). However, these perturbations are very small, due to the extreme stiffness of spacetime. To obtain a sense of the stiffness of spacetime we can compare the rigidity of spacetime to the Youngs modulus of diamond. The rigidity of spacetime is 10^{19} Pa, which is 10^7 times larger than the Youngs modulus of diamond at 10^{12} Pa [3]. Even the small perturbations we hope to observe are caused by extremely violent astrophysical events.

Sources of gravitational waves are some of the most energetic events known to exist in the universe. The primary expected source of gravitational waves for LISA is a compact binary system, such as two inspiraling black holes, or neutron stars, as in Figure 2. The inspiraling bodies can be modeled precisely using general relativity and produce a characteristic "chirp" signal. The chirp consists of a gravitational wave signal increasing in amplitude and frequency up to the point where the binary coalesces. Near coalescence, the gravitational wave signal becomes complicated before ringing down as the system settles into a new black hole (Figure 3).

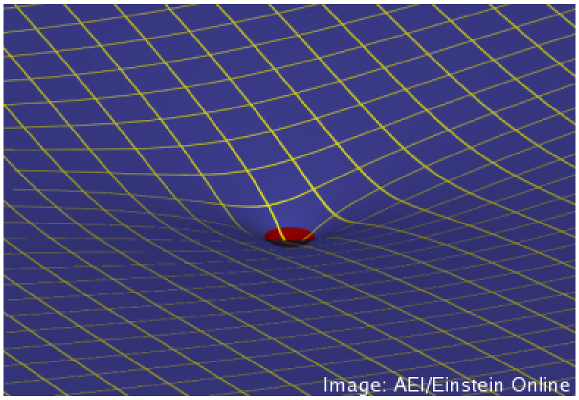

Figure 1. Spacetime is bent by a massive body trapping smaller masses. Image courtesy of the AEI/Eienstein Online.

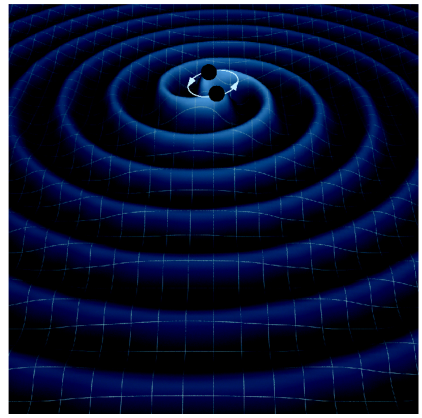

Figure 2. Certain motions of massive bodies, such as black holes, may cause waves in spacetime. Image courtesy of K. Thorne (Caltech) and T. Carnahan (NASA GSFC).

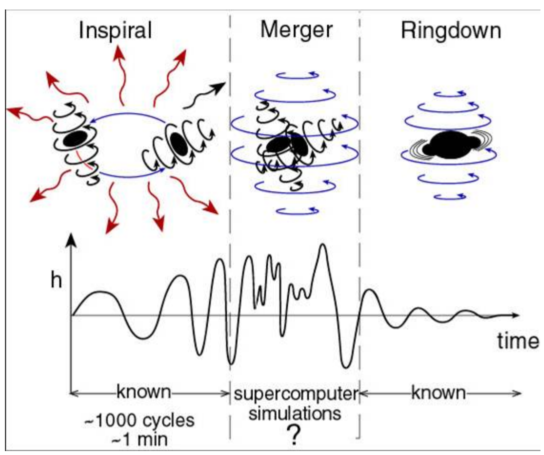

Figure 3.
Characteristic chirp signal from a compact binary inspiral. Three distinct stages: the chirp, a complicated coalescence, and a ring down. Kip Thorne (CalTech)

Other sources of gravitational waves include the absorption of a lesser body by a black hole, so-called black hole dining events, which may emit gravitational waves during the bodies' decaying orbit [1, 2]. The gravitational wave signal from the decaying orbit should allow for the precise mapping of the strong gravity field of a black hole. Gravitational waves may also come from supernovae with sufficient asymmetry, and from spinning neutron stars with small distortions of their surface [4]. Additionally, a few more exotic phenomena are expected to radiate gravitational waves, such as cusps formed by cosmic strings and the big bang [2].

Gravitational waves offer a different view of the universe than electromagnetic radiation. When we observe astrophysical objects and events in the electromagnetic spectrum, we are seeing these events through a veil of interstellar gas and dust. Since photons are strongly interacting, they are scattered, absorbed, and reemitted by the intervening dust. Thus, we see emission and absorption lines corresponding to the make-up of the intervening medium, not the radiation emitted from the original source. Gravitational waves, on the other hand, are weakly interacting and travel through intervening dust unperturbed. Thus, gravitational waves allow us to observe a more pure picture of the emitting object or system [1]. While the weakly interacting nature of gravitational waves retains the purity of the signal, it also makes detection very difficult, since interaction with the detector will also be weak.

In order to understand how we might approach detecting gravitational waves, it is useful to understand how they interact with matter, of which our detector will be constructed. The effect of a gravitational wave on a spatially extended system is particularly easy to observe by the interaction of a gravitational wave with a ring of massive particles (Figure 4). For a gravitational wave passing through the plane of the page, the ring of particles will alternately expand and contract along orthogonal axes [4].

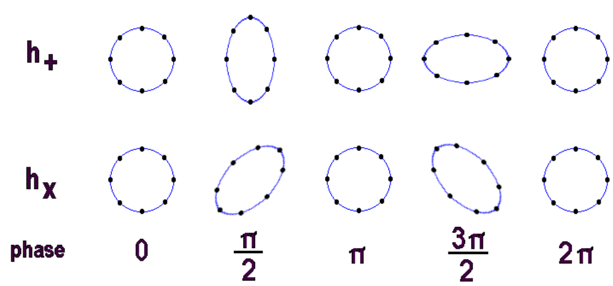

Figure 4. The effect of a gravitational wave that is traveling perpendicular to the plane of the page, upon a ring of particles. The two polarizations *plus* and *cross* are shown. Wm. Robert Johnston, UT Dallas

The weak interaction of a gravitational wave is expressed in terms of a unitless strain $h = \Delta L/L$; where, for LISA gravitational wave sources $h > 10^{-23}$. Thus, for a length $L = 5 * 10^9$ meters between two masses, for example the diameter of the above ring, a continuous gravitational wave with a strain of 10^{-23} will cause a sinusoidal displacement of $\Delta L = 5 * 10^{-14}$ meters. In comparison, the radius of an atom is about an angstrom, or 10^{-10} meters. Though these displacements are tiny, it is thought that they are detectable with about a year of observations. Several ground-based detectors are now in operation, and a space-based mission, LISA, is currently in development. A significant benefit of a space-based detector is that the length L can be made much larger than for any ground-based detector, thus increasing the detector sensitivity.

2.2. LISA

The fundamental idea of a space-based detector is to place a system of proof masses (PM) in space, to allow them to follow the natural curvature of spacetime, paths called geodesics, and to measure the variations in distance between them. In order to measure the small motions of the PMs due to gravitational waves, or other disturbing effects, a spacecraft can be positioned about each mass using drag-free technology. The spacecraft may then carry out the measurements of the motions between different PMs using interferometry. This is essentially what LISA aims to accomplish, though the implementation is more complicated.

LISA consists of a constellation of three identical spacecraft, nominally arranged in an equilateral triangle, in a helio-centric orbit at 1 A.U. (Figure 5). The configuration is equivalent to two interferometers sharing one arm, where each arm is 5 million kilometers long. The plane of the LISA constellation is oriented 60 deg to the ecliptic, and the center of the constellation is proposed to lag the earth by 20 deg. Parameters for the LISA orbit were chosen for reasons relating to the orbital mechanics and to balance between the disturbing effects of earth's gravity field, the propulsion requirement to establish the orbit, and the communications power needed to reach earth [5].

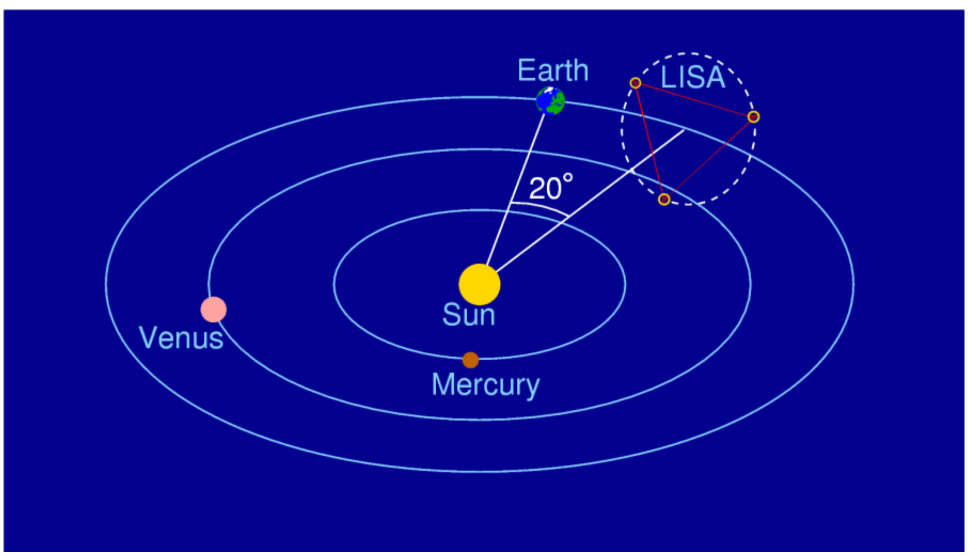

Figure 5. LISA constellation and orbit. Image courtesy of the LISA science team.

Laser interferometry in LISA will be done between each pair of spacecraft in a rather unconventional sense, since due to extremely long interferometer arms the intensity of the laser light arriving from the distant spacecraft is quite low [5]. Thus, rather than bouncing laser light off of a distant mirror, as would be done in a conventional interferometer, each spacecraft houses its own laser. The local laser is phased-locked to incoming laser light from the distant spacecraft, and then returns an identical signal to the distant spacecraft at full power.

Although the constellation consists of three spacecraft, there are actually two PMs per spacecraft. Each PM is encased in a housing that is secured to an optics bench on the spacecraft; thus, two optics benches are arranged in a Y-configuration on each spacecraft (Figure 6). Motions of the PMs are detected both optically, using interferometric techniques, and capacitively, with capacitive sensors on the inside of each housing [5, 6]. Motion of the PM relative to the spacecraft creates a displacement signal, which then informs the spacecraft thrusters to maintain correct spacing of the spacecraft about each PM.

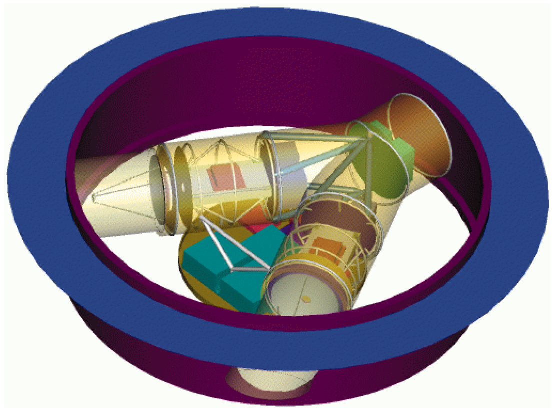

Figure 6. One of three spacecraft. Pictured with the solar panels removed. A Y-like configuration of two optics benches holding laser ranging equipment as well as housing for PMs. Image courtesy of the LISA science team.

Gravitational waves are not the only force perturbing the PM [7, 8]. In addition to the gravitational wave perturbations, there are many sources of spurious acceleration on the PMs and spacecraft. The primary source of spurious accelerations on the spacecraft is from variations in the solar radiation flux [8]. Additional contributions to spurious spacecraft accelerations come from the variations in the solar wind, and to a smaller extent from micro meteor impacts. Many spurious sources also cause direct accelerations to the PMs. One such source comes from charging by cosmic rays, inducing a net charge on the PMs, which in turn may interact with both interplanetary magnetic fields and stray electromagnetic fields on the spacecraft. Additionally, significant accelerations of the PMs may be caused by variations in the local gravity field, which result from rotating the communications antenna.

The spacecraft serves to protect the PM from external sources of disturbance. To do this it must maintain the position of the PM within. Sensing of the PM position is achieved with a capacitive measurement between the PM and capacitor plates on the inside of the PM housing (Figure 7). It will also be necessary to impart small electrical forces to the PM in order to compensate for known disturbances. This to is achieved by applying a voltage across the capacitor plates within the housing and electrostatically forcing the PM.

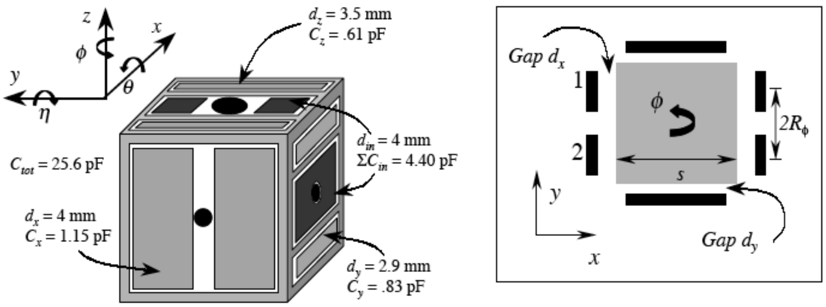

Figure 7. Capacitive sensors on housing surrounding proof mass. The proof mass is planned to be gold-platinum cube 46 mm per side and 2 kg in mass. Image courtesy of W. J. Weber, Universita di Trento [9].

3. Voltage Stability

3.1. Problem Statement

The GRS for LISA is expected to be similar to those being flown on the LISA Pathfinder mission. Each GRS consists of a PM enclosed within a housing which has capacitor plates on the inside (Figure 7). The gap between the capacitor plates and the surface of the PM is about 4 mm. These capacitor plates are used to apply electrical forces to the PM, as needed, and to sense relative motions of the PM housing system.

Although external spurious forces are compensated for by the spacecraft thrusters, some small forces must still be applied to the PMs. This is because there will be slightly different forces and torques acting on the two PMs within each spacecraft. To keep each PM from drifting away from the center of its housing, compensating electrical forces must be applied along some axes.

This research addresses the question of how low the noise in the applied voltages can be kept, which is expected to be determined mainly by the stability at frequencies down to 0.1 mHz of the dc voltage references that are used. Measurements of voltage stability for a few commercially available voltage references had been made previously by Gerhard Heinzel et al at the Max-Planck Institute for Gravitational Physics in Hannover Germany, [10]. This measurement demonstrated relative noise levels of $1 * 10^{-6}/\sqrt{Hz}$ at 0.1 mHz with moderate temperature stabilization. We investigate whether the noise level will improve with better thermal stability.

3.2. Experimental set-up and circuit

We have measured the low frequency stability of voltage references in a similar way to Heinzel et al, by comparing two identical voltage references. Voltage references were compared using a differential amplifier within a temperature controlled environment. The apparatus is a double walled box lined with insulating foam and tin foil (Figure

8). The outside of the box is wrapped in plastic to minimize air exchange between the room and the insulating air gap between box walls. Temperature control is achieved via heating thermal mass (specify quantity) within the enclosure. A heater is controlled by a servo loop to keep the temperature at a desired level within the enclosure. The servo loop reads from one of two sensors within the enclosure, whose positions are shown in figure 8. The temperature in the laboratory is also monitored. Temperature stabilities of approximately $5mK/\sqrt{Hz}$ at 10^{-4} Hz were obtained, which is approximately a factor of 1000 better than laboratory conditions

A circuit topology was designed for testing multiple voltage references in identical conditions. The topology consists of several test boards arrayed of a central power bus, as in Figure 9, and is fitted with a pair of voltage references. Each test board contains a differential amplifier that is used to compare the outputs of two voltage references (Figure 10). The differential amplifier is centered around an operational amplifier (opamp), which is the primary source of background noise on the test board. The opamp used in the differential amplifier circuit was chosen to have a high input impedance, low temperature coefficient, and low noise output. A high input impedance limits the amount of current sourced by the voltage references, which operate at a lower noise level at lower output current (How and Why?). The best characteristics were obtained with an OP07CP.

3.3. Circuit characterization

To characterize the noise of each test board without voltage references the inputs to the opamp were shorted to ground (how does this get around common mode rejection). The noise of the empty circuit at 10^{-4} Hz was typically found to be $0.5\mu V/\sqrt{Hz}$ using an OP07CP opamp (Figure 11).

The temperature sensitivity of the test board was measured by driving the heater with a sinusoidal signal, causing the temperature in the enclosure to vary accordingly. The ratio of the noise of the circuit at the driving frequency to the temperature stability within the enclosure gives us the temperature dependence of the test board. Th primary source of this noise is thought to be the opamp. (do my measurements match with specs?)

$$t = \frac{\tilde{V}(f_{driving})}{\tilde{T}(f_{driving})} \tag{1}$$

Where t is the temperature dependence, and where $\tilde{V}(f)$ and $\tilde{T}(f)$ are the stabilities of the output voltage and enclosure temperature respectively.

Additional tests of the test board noise were done by applying a generated gaussian noise signal to the inputs and comparing the output noise to the raw generated input noise. The noise at the output is divided by the gain of the amplifier to attain the equivalent noise at the inputs. (More about this??)

The amplifier gain is set to amplify the difference in voltage between voltage references above the noise level of the test board and data acquisition system. Typically

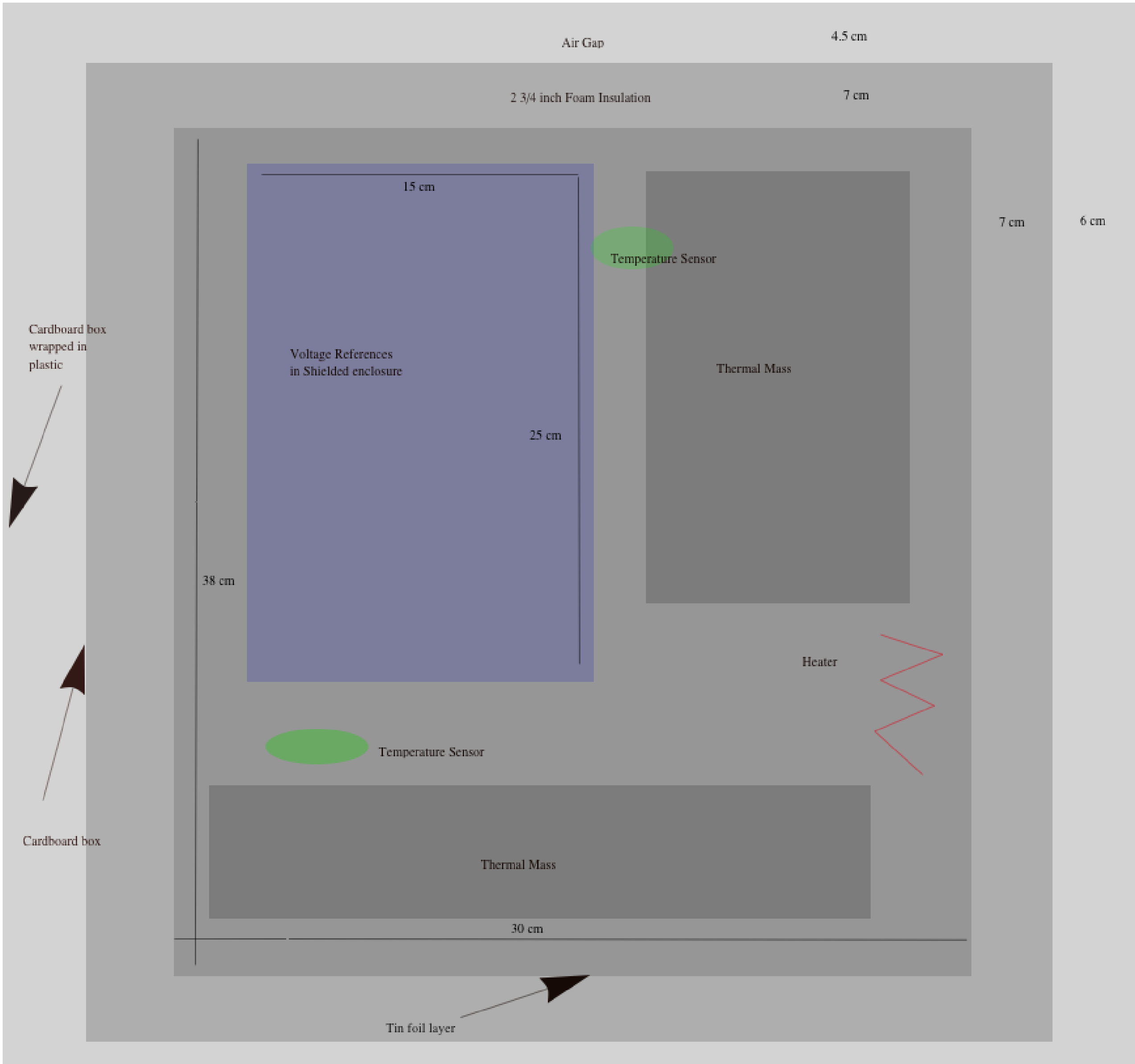

Figure 8. Experimental setup geometry showing double layered box with air gap, foam insulation, and tin foil. A power supply was also placed within the enclosure, which acts as more heating power and provides thermal stability to the power supply. Relative positions of heater and temperature sensors is also shown.

this was chosen to be $G \approx 4000$. The gain of the differential amplifier is set by the choice of resistors, which are usually chosen in pairs $R_1 = R_2$ and $R_3 = R_4$, where $G = R_1/R_3$ (Appendix A), such that

$$V_{out} = -G * (V_{in-} - V_{in+}) \tag{2}$$

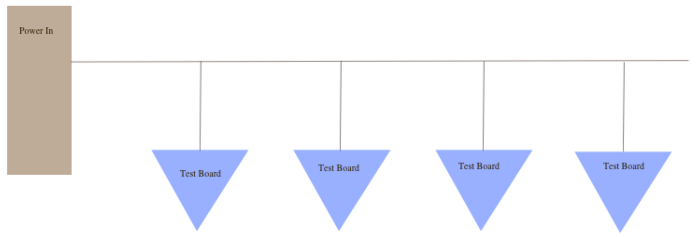

Figure 9. Multiple test board circuit topology.

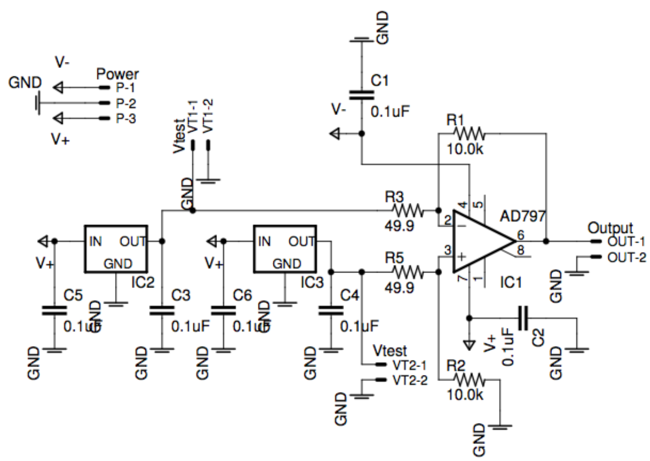

Figure 10. Test board containing differential amplifier circuit. IC1 is an op-amp, IC2 and IC3 are voltage references. Filtering capacitors shown. Schematic courtesy of Michael Nickerson, University of Colorado, JILA

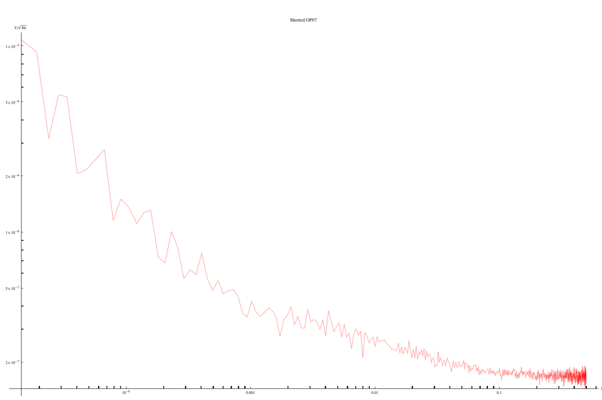

Figure 11. Characteristic circuit noise with a shorted OP07CP operational amplifier.

3.4. Measurements and Analysis

I present estimated values for the noise levels of several voltage references at 10^{-4} Hz. These are raw values from the output time series. Additional sources of noise are thought to be negligible, these will be discussed below.

We perform spectral techniques on the output time series to obtain an amplitude spectral density function. The amplitude spectral density is the square root of the power spectral density, or just the magnitude of the Fourier transform, $a(f) = \sqrt{P(f)} = |s(f)|$. To estimate the amplitude spectral density we take the absolute value of the discrete Fourier transform of the time series V_t,

$$|v_s| = |\frac{1}{\sqrt{N}} * \sum_{t=1}^{N} V_t * e^{2*\pi i(t-1)(s-1)/N}| \tag{3}$$

Corresponding frequencies are computed as integer multiples of the bandwidth $BW = 1/(\tau * N)$ where τ is the sample time and N is the number of points. Hence we obtain the amplitude spectral density by constructing the data table (pairwise function) $a(f) = (s * BW, |v_s|)$, plotted in figure 12.

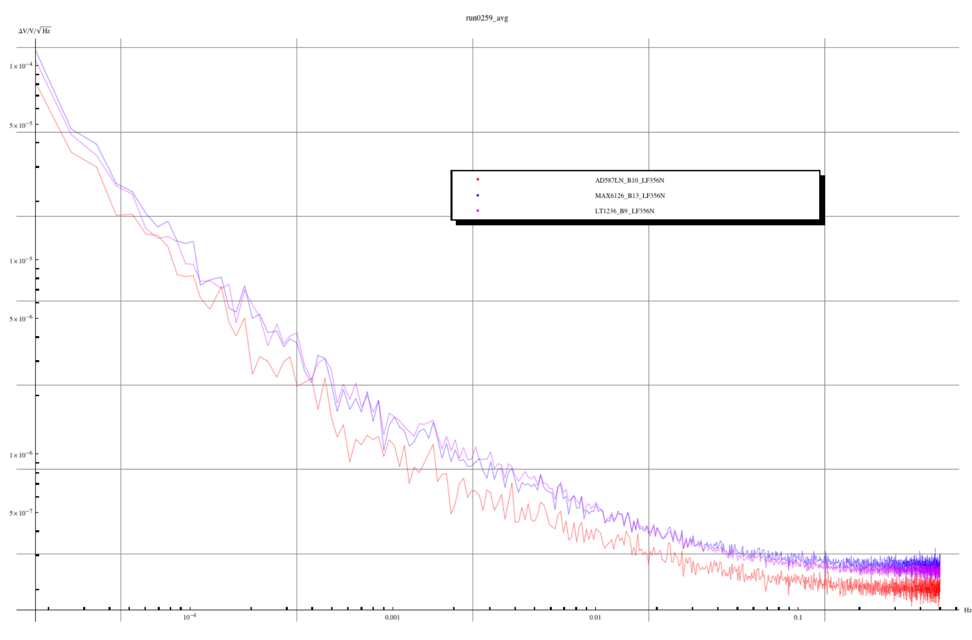

Figure 12. This is a place holder –data on the way! "Money Plot"

The equivalent noise level at the inputs of the differential amplifier is calculated by taking $a(f)/G$. This is the quadrature sum of the noise of two voltage references, and is what we present. Assuming that the voltage references are independent and uncorrelated the noise of each voltage reference can be estimated by dividing our estimated values by an additional factor of $\sqrt{2}$.

The results are summarized in Table 1. To estimate the noise level at 10^{-4} Hz the mean value from each data run is estimated by computing the mean value of the amplitude spectral data within a $2*BW$ window centered on 10^{-4} Hz. This amounts to averaging three data points, the one lying closest to 10^{-4} Hz and the point on each side. We then compute a weighted average of the estimates from individual runs to obtain an overall estimate. The weights are determined by the square root of the length of the run, $w_i = \sqrt{N_i}/\Sigma_j\sqrt{N_j}$, where N_i is length of the the ith run. Errors are determined from the standard deviation.

Note that a different weighting scheme, where the weights were determined according to the length of the data run $w_i = N_i/\Sigma_j N_j$ was also investigated. However no appreciable difference was found. Furthermore, the average using the first weighting scheme lies between the evenly weigthed mean and that computed in the linear weighting scheme.

Table 1. Raw Voltage Reference Noise Levels ("Money Table")

Voltage Reference	Output voltage [Volts]	OP07 level [$ppm/\sqrt{Hz}$]	Number of measurements
AD587LN	10	level ± error	level
LT1236	10	level ± error	level
LT1021	5	level ± error	level
MAX6162	5	level ± error	level

Many voltage references were tested in earlier versions of the apparatus and at room temperature. Those that performed weakly were not further measured in subsequent versions of the apparatus. The following voltage references were found to have rather poor stability at 10^{-4} Hz: AD423, AD680, Ref102 (Burr Brown).

3.5. Environmental Noise Sources

Here we discuss the known noise sources. Each voltage reference is temperature dependent. As with the temperature dependence of the test boards this is measured by driving the enclosure temperature strongly at a known frequency and comparing the noise level of the reference to the temperature stability at the driving frequency. We find that the temperature dependence of the voltage references is on the order of 10^{-6} V/ K. Hence, for a temperature stability of $10mK\sqrt{Hz}$, this is a negligible effect.

Voltage references are also sensitive to power supply fluctuations, a measure called line regulation. The line regulation determines how much the output voltage will vary for a given variation in power supply voltage. The line regulation is typically small, below $\pm100\mu V/V$. Thus, for maximum power supply stability of $5mV/\sqrt{Hz}$ at 10^{-4} Hz this results in noise of $0.5\mu V/\sqrt{Hz}$.

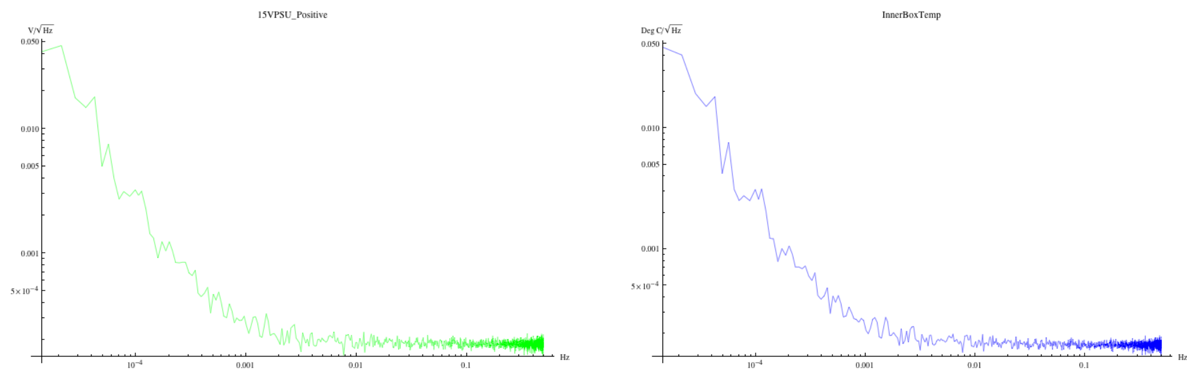

Figure 13. Stability of 15 V power supply and inner box temperature.

4. Conclusions

We characterized the noise of voltage references at low frequencies in a similar manner to Heinzel et al. and demonstrated consistent results for a AD587LN voltage reference. Additionally, we have tested a number of other voltage references and measured their temperature dependencies. Additionally, we have found that further temperature stabilization will have minimal effect on lowering the voltage reference noise. Thus, though the space environment will be more temperature stable than our laboratory, we have determined that the voltage stability will not be strongly affected.

5. Appendices

5.1. Appendix A: Differential amplifier gain

We write down the current at each node, and use the relation for an op-amp $V_- = V_+$ to solve for the output voltage V_{out} in terms of other quantities.

Non-inverting node:

$$I_+ = (V_{in+} - V_+) * \frac{1}{R_1} \tag{4}$$

$$= \frac{V_+}{R_2} \tag{5}$$

Thus,

$$V_+ = \frac{R_2 * V_{in+}}{R_1 + R_2} \tag{6}$$

Inverting node:

$$I_- = (V_{in-} - V_-) * \frac{1}{R_1} \tag{7}$$

$$= \frac{1}{R_2} * (V_- - V_{out}) \tag{8}$$

but $V_- = V_+$ so,

$$\frac{1}{R_1} * (V_- - \frac{R_2 * V_{in+}}{R_1 + R_2}) = \frac{1}{R_2} * (\frac{R_2 * V_{in+}}{R_1 + R_2} - V_{out}) \tag{9}$$

Solve for V_{out}, but we for ease of calculation we will make the substitution $G_1 = 1/R_1$ and $G_2 = 1/R_2$. Then,

$$G_1 * V_{in-} - \frac{G_1^2 * V_{in+}}{G_1 + G_2} = \frac{G_1 * G_2 * V_{in+}}{G_1 + G_2} - G_2 * V_{out} \tag{10}$$

$$-G_2 * V_{out} = G_1 * V_{in-} - V_{in+} * (\frac{G_1^2 + G_1 * G_2}{G_1 + G_2}) \tag{11}$$

Which simplifies to:

$$-G_2 * V_{out} = G_1 * (V_{in-} - V_{in+}) \tag{12}$$

Thus,

$$V_{out} = -\frac{G_1}{G_2} * (V_{in-} - V_{in+}) \tag{13}$$

or, in terms of the resistances

$$V_{out} = -\frac{R_2}{R_1} * (V_{in-} - V_{in+}) \tag{14}$$

5.2. Appendix B: Temperature sensor calibration

Temperature measurement plays a fairly significant role in the noise analysis. We calibrated our temperature sensor by comparing it with another temperature sensor in various temperature baths.

Both the pre-calibrated sensor and sensors being tested were placed in various temperature baths: a cup of ice, above ice water, in a cup of cold water, and at room temperature. The sensors were allowed to come to equilibrium with the environment, then voltages were read off the sensors being tested while a temperature was read from the pre-calibrated sensor. The range of environments was chosen to obtain a broad spread in temperatures and hence a more accurate slope of volts/deg C. A linear fit of the data is performed by Mathematica. The results for one sensor are shown below.

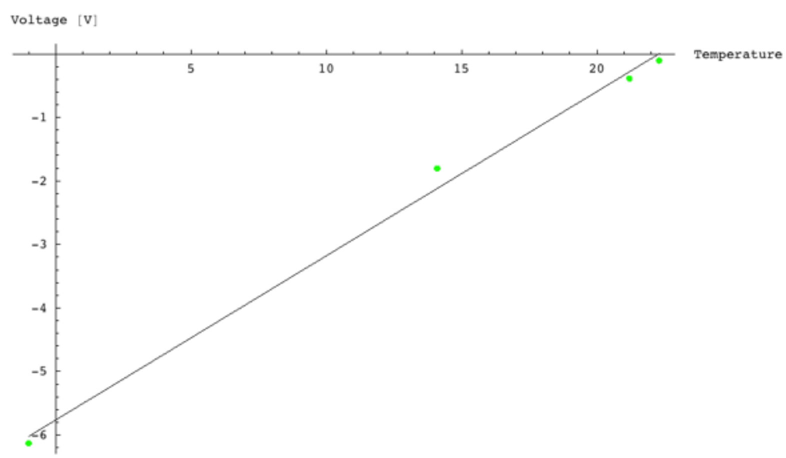

Figure 14. Calibration of a temperature sensor using a pre-calibrated sensor.

6. Bibliography

[1] S. Hawking and W. Israel, editors, *300 Years of Gravitation* (Cambridge University Press, 1987).
[2] C. J. Hogan, (2007), arXiv:0709.0608 [astro-ph].
[3] S. Pollock, *Analytic and Interferometric Techniques for the Laser Interferometer Space Antenna*, PhD thesis, University of Colorado Boulder, 2005.
[4] P. R. Saulson, *Fundamentals of Interferometric Gravitational Wave Detectors* (World Scientific, 1994).
[5] J. Baker *et al.*, LISA: Probing the universe with gravitational waves, 2007.
[6] P. Bender, Classic and Quantum Gravity **23**, 6149 (2006).
[7] T. Stebbins *et al.*, Classic and Quantum Gravity **21**, 653 (2004).
[8] B. L. Schumaker, Classic and Quantum Gravity **20**, 239 (2003).
[9] M. Cruise and P. Saulson, editors, *Gravitational-Wave Detection* Vol. 4856, SPIE, 2003.
[10] J. C. L. Stephan Mirkowitz, editor, *Components for the LISA local interferometry*, 6th International LISA Symposium, AIP, 2006.